

RSC Advances



This is an *Accepted Manuscript*, which has been through the Royal Society of Chemistry peer review process and has been accepted for publication.

Accepted Manuscripts are published online shortly after acceptance, before technical editing, formatting and proof reading. Using this free service, authors can make their results available to the community, in citable form, before we publish the edited article. This *Accepted Manuscript* will be replaced by the edited, formatted and paginated article as soon as this is available.

You can find more information about *Accepted Manuscripts* in the [Information for Authors](#).

Please note that technical editing may introduce minor changes to the text and/or graphics, which may alter content. The journal's standard [Terms & Conditions](#) and the [Ethical guidelines](#) still apply. In no event shall the Royal Society of Chemistry be held responsible for any errors or omissions in this *Accepted Manuscript* or any consequences arising from the use of any information it contains.

Cite this: DOI: 10.1039/c0xx00000x

www.rsc.org/xxxxxx

ARTICLE

Electrospun Composite Nanofibres of PVA Loaded with Nanoencapsulated n-Octadecane

Sidharth Sirohi, Dharendra Singh, Ratyakshi Nain, Dambarudhar Parida, Ashwini K. Agrawal* and Manjeet Jassal*

Received (in XXX, XXX) Xth XXXXXXXXX 20XX, Accepted Xth XXXXXXXXX 20XX
DOI: 10.1039/b000000x

In this study composite nanofibres of PVA consisting of polystyrene/n-octadecane nanocapsules were prepared. The n-octadecane present as core of nanocapsules acts as phase change material (PCM) for thermal storage properties. Controlled size nanoencapsulated PCMs were prepared by surfactant free RAFT miniemulsion polymerization of styrene. These nanocapsules were incorporated into nanofibres by electrospinning a mixture of nanocapsule latex containing octadecane as core and polystyrene (PS) as shell material with aqueous solution of poly(vinyl alcohol). The morphology and thermal properties of resultant PVA nanofibres were studied by field emission scanning microscopy (FE-SEM), scanning transmission electron microscopy (STEM), high resolution transmission electron microscopy (HRTEM) and differential scanning calorimetry (DSC). The composite nanofibres could show latent heat storage capacity of approx. 4-5 J/g. This method offers opportunity to produce low diameter composite nanofibres with uniform dispersion of encapsulated material for various applications.

1. Introduction

Electrospinning provides a simple straight forward, cheap and unique approach for production of polymeric nanofibres in the range of 1000 nm or less.¹⁻⁵ The advantages of electrospinning include production of ultrathin fibres with large surface area and superior mechanical properties.⁶⁻⁹ These outstanding properties have made electrospun webs promising candidates for various applications. These include filtration,¹⁰ fuel cells,¹¹ nanowires,¹² catalyst supports,¹³⁻¹⁴ chemical and biological protection suits¹⁵, drug delivery devices,¹⁶ nanodevices,¹⁷ nanocomposites,¹⁸ and tissue scaffolds.¹⁹ The electrospinning of polymer solutions with particles,²⁰ nanotubes or proteins embedded in them has been reported in the literature.²¹⁻²² The electrospinning of composite nanofibres loaded with capsules have also been reported.²³⁻²⁴ However, the diameter of these composite nanofibres was observed to increase to micron range due to the large size of the loaded capsules and inhomogeneity in their dispersions.²⁵ Such systems are important for applications where handling of encapsulated sensitive materials such as biomolecules and catalysts is critical. The preparation of uniform size nanocapsules and their uniform dispersion for their optimum loading in nanofibres remain as some of the major challenges and require further investigation.

In this study, we have used electrospinning technique to produce composite PVA nanofibres loaded with controlled size

nanoencapsulated PCMs. The PCMs of 97 nm size were prepared in our laboratory by surfactant free RAFT miniemulsion polymerization using co-oligomer of styrene and maleic anhydride (SM-RAFT) as amphi-RAFT agent. SM-RAFT was synthesized by RAFT polymerization using phenylethyl dithioacetate (PEPDA) as the RAFT agent. The SM co-oligomer acted as an emulsifier and RAFT agent for controlling size of nanocapsules in miniemulsion. The influence of controlled size of NCs on the final diameter of composite nanofibres was investigated. Experiments were also conducted to optimize loading of PCM nanocapsules (NCs) in PVA nanofibres.

2. Experimental Work

2.1 Materials

Styrene (Merck, Germany) was distilled prior to its use and azobisisobutyronitrile (AIBN) was recrystallized twice in methanol. Maleic anhydride (Aldrich, USA), potassium persulphate (KPS) (Merck, India), n-octadecane, (90%, Spectrochem, India), poly(vinyl alcohol) (cold, avg. mol. wt. 1,24,000, degree of alcoholysis 80%) (Aldrich, USA), n-hexane (Spectrochem, India), and ammonia solution (25% w/v) (Merck, India) were used as obtained. The n-octadecane was used as phase change material with transition temperature of 298 K and latent heat of 215 J/g.

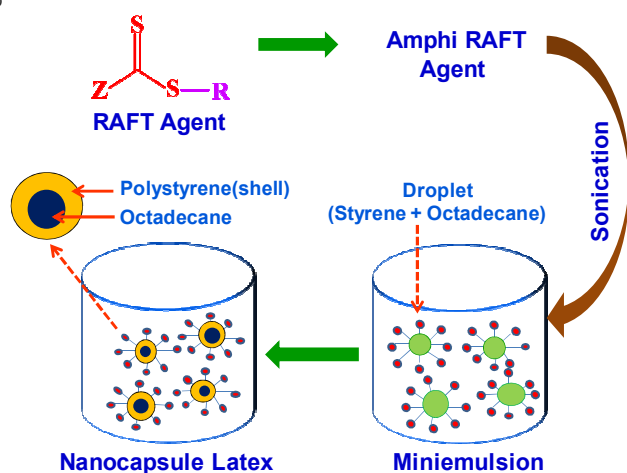
2.2 Preparation of polystyrene /n-octadecane nanocapsules

The PS/n-octadecane NCs were prepared by surfactant free RAFT miniemulsion polymerization using amphiphilic co-oligomer of styrene and maleic anhydride (amphi-RAFT agent) (Scheme 1). The co-oligomer was synthesized using phenylethyl phenyl dithioacetate (PEPDA) as RAFT agent and AIBN as initiator. For this, Sty: MAn:PEPDA:AIBN ratio of 225 : 25 : 5 : 1 was taken and the reaction was carried out at 60 °C for 130 minutes. The co-oligomer was obtained by precipitation of reaction mixture in methanol which was further dried at 50 °C in vacuum oven overnight.

Table 1. Characteristics of SM co-oligomer.

Co-oligomer	Avg. M_n (Theo.)	Avg. M_n (Cal.)	M_w/M_n	T_g (°C)	CMC (mg/ml)
SM-84	2073	1998	1.3	111	0.1584

For preparation of polystyrene/n-octadecane NCs, aqueous solution of ammonia (0.5% w/v) was added to mixture of styrene, macroRAFT agent (amphi-RAFT agent), n-octadecane and deionized water. The mixture was initially stirred for 20 minutes at 60 °C then subjected to ultrasonication for 10 minutes at 50 °C. The mixture was further stirred at 60 °C for 60 minutes and finally sonicated for 15 minutes to complete the hydrolysis of anhydride units. The obtained miniemulsion was transferred to 25 ml two necked round bottom flask and kept in N_2 purging for 15 minutes. The polymerization was initiated by injecting aqueous solution of potassium per sulphate. The reaction was continued for 5 hours at 68 °C. The nanocapsule latex prepared by RAFT miniemulsion polymerization was used for preparation of composite nanofibres using electrospinning.

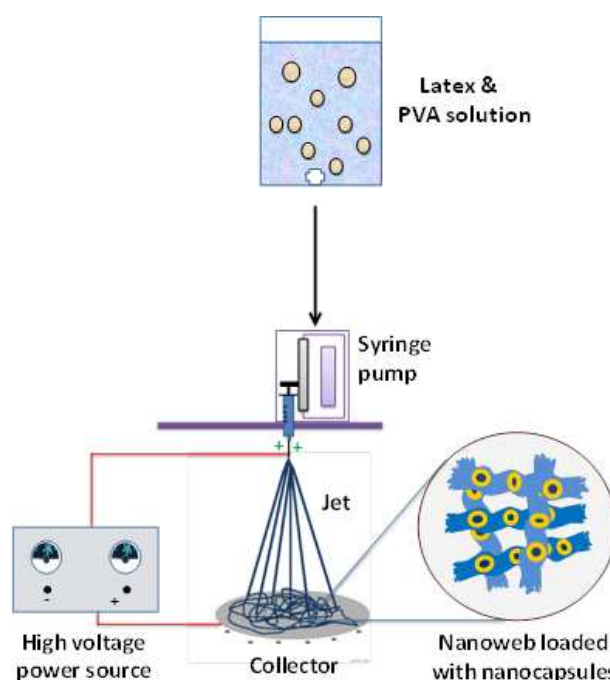


Scheme 1. Procedure of PS/OD NCs preparation.

2.3 Electrospinning

A 14% (w/w) homogeneous dope solution of PVA in DI water was prepared by stirring required quantity of polymer at 80 °C for 4 hours. Polystyrene nanocapsule latex containing octadecane as

core material was added to 14% PVA solution so as to adjust concentration of octadecane to 10%, 15% and 20% on the weight of PVA. The dopes were stirred for 2 hours prior to electrospinning. Nanofibres were electrospun at minimum electrospinning voltage (MEV). MEV is defined³ as the minimum electrospinning voltage required for complete conversion (or maximum possible conversion for dilute solutions). MEV is determined as per the reported method.⁵ The electrospinning was carried out using an infusion syringe pump (KDS 100 from KD Scientific, Massachusetts USA) with a flat tip needle (inner diameter of 0.84 mm) as the spinning head and 40 kV high voltage supply (DES 40 PN from Gamma high voltage, Florida, USA). The distance from the tip of the needle to the collector was kept as 15 cm and a flow rate of 0.25 ml/h was used. A stainless steel disc was used as collector and aluminium foil was used as a substrate (Scheme 2). The applied needle voltage for electrospinning was 10-13 kV.



Scheme 2. Schematic of electrospinning set up.

2.4 Characterization

¹H NMR of co-oligomer. ¹H NMR was performed on a 400 MHz (JEOL, Tokyo Japan) spectrometer at room temperature using $CDCl_3$ and tetramethylsilane as an internal standard. Experiments were conducted using relaxation delay time of 5s.

Electron Microscopy The surface morphology of NCs and their composites with PVA were characterized by FE-SEM Quanta 200F (Eindhoven, The Netherlands) and HRTEM, JEOL (Tokyo, Japan). The diameter of the nanofibres was measured using Image J software (NIH, USA). Diameter of 100 fibres was measured and an average value with standard deviation has been reported for all the samples.

Fourier transform infrared spectroscopy (FT-IR). FT-IR analysis of dried PVA nanofibres webs was performed on FT-IR

spectroscopy model spectrum BX from Perkin Elmer (Waltham, USA). All spectra were collected with a 2 cm^{-1} wave number resolution.

Differential scanning calorimetry (DSC). The capsules were dried by lyophilizer (Labconco, Kansas USA) and washed with hot water to remove physically adhering OD before analysis. The loaded nanofibre webs were washed with n-hexane to remove physically adhering capsules on the web and dried under vacuum at $50\text{ }^{\circ}\text{C}$ prior to DSC analysis, which was performed on Q200 DSC from TA Instruments (New Castle, USA). The samples were equilibrated at $-20\text{ }^{\circ}\text{C}$ then heated to $50\text{ }^{\circ}\text{C}$ at rate of $10\text{ }^{\circ}\text{C}/\text{min}$ under nitrogen atmosphere.

3. Results & Discussion

3.1 SM-RAFT co-oligomer

The ^1H NMR spectrum of co-oligomer is shown in figure 1. The chemical shift appeared at 6-7.5 ppm represents aromatic hydrogens of styrene while broad peak at 1-4.0 ppm shows presence of methine protons of maleic anhydride ($\delta = 2.5\text{-}4.0\text{ ppm}$) and methine/methylene protons of styrene units ($\delta = 1.0\text{-}2.5\text{ ppm}$) of co-oligomer.

FT-IR spectrum of co-oligomer is shown in figure 2. The broad peak between $3000\text{-}3100\text{ cm}^{-1}$ corresponds to aromatic C-H stretching in co-oligomer and the peak between $2850\text{-}2975\text{ cm}^{-1}$ corresponds to aliphatic C-H stretching while peaks at 1775 and 1853 cm^{-1} were due to anhydride group stretching of maleic anhydride present in the co-oligomer.

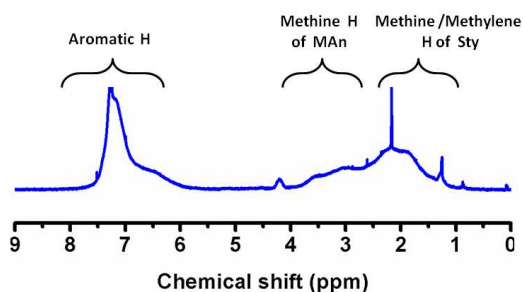


Figure 1. ^1H NMR spectrum of co-oligomer.

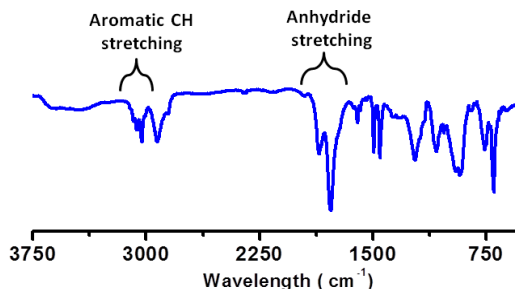


Figure 2. FT-IR spectrum of co-oligomer.

3.2 Morphological study and thermal analysis of NCs

HRTEM and FE-SEM micrographs of NCs, shown in figure 3,

revealed both filled NCs and unfilled polystyrene particles in the latex NCs. The TEM micrographs of NCs latex confirmed the presence of large number of octadecane (OD) filled polystyrene NCs consisting of well defined core shell structures with average diameter $97 \pm 33\text{ nm}$. The OD is seen as lighter density core surrounded by dense polymeric wall. The average diameter of core of NCs was 31 nm and shell thickness was found to be 17 nm . The encapsulation efficiency was 80%.

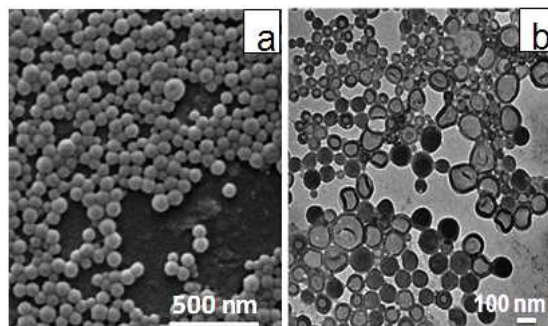


Figure 3. FE-SEM and HRTEM micrographs of PS/OD NCs.

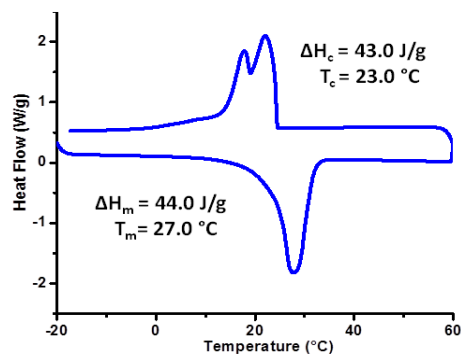


Figure 4. DSC thermograph of PS/OD NCs.

The DSC graph is shown in figure 4. The absorption (endothermic transition) and release of heat (exothermic transition) of the NCs loaded with n-octadecane were observed at 27.0 and $23.0\text{ }^{\circ}\text{C}$, respectively. The latent heats of these transitions were nearly same at 44.0 and 43.0 J/g , respectively. From the latent heat values, the core content of the capsules was calculated to be $\sim 20\%$, which is high considering the small size of the NCs.

3.3 Electrospinning of composite nanofibres loaded with PS/OD nanocapsules

The electrospinning of control PVA (14% w/w) was smooth and continuous. Our group has recently reported the influence of polymer elasticity and other electrospinning parameters such as spinning distance and flow rate on morphology of nanofibres based on PAN/DMF^{3,5,26-27} and PVA/water systems.⁴ It was found that when PVA was electrospun at MEV, the diameter of the nanofibres did not change significantly with either the spinning distance or the flow rate. However, the polymer rheology had a great influence because of the change in elasticity

of the system. The concentration of PVA, which influences the solution rheology, changes the diameter of the nanofibres. The addition of nanocapsule latex into PVA solution resulted in dilution of PVA from 14 wt% solution. Because of this dilution, the diameters of nanofibres were found to change and are reported in Table 2. NCs equivalent to 10 to 20 wt% of OD on the weight of PVA were incorporated during electrospinning. A resultant PVA solution of 8.3 wt% was obtained after incorporation of 20 wt% OD. However, the diluted solution had sufficient viscosity for continuous spinning. 10 and 15 wt% of OD loading did not affect the spinning behaviour of PVA and the spinning was still continuous and yielded good quality fibres. However on increasing the OD loading to 20 wt%, the spinning was found to be intermittent. The nanofibre webs were washed with n-hexane to remove physically adhering NCs present on the surface of the nanofibres before further characterization.

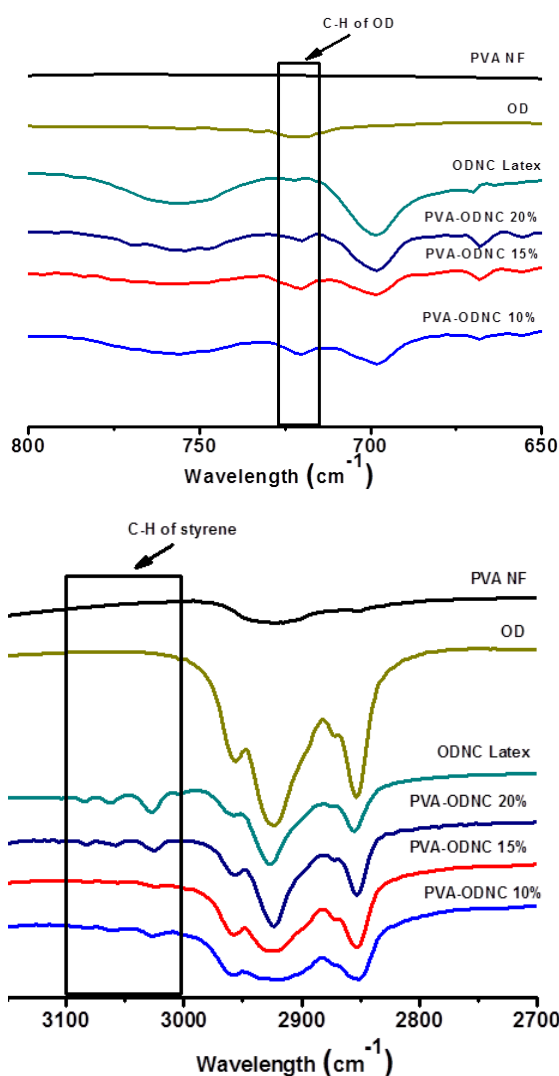


Figure 5. FT-IR spectra of PVA nanofibres (PVA NF), octadecane (OD), octadecane nanocapsule latex (ODNC), PVA-octadecane latex (PVA-ODNC) at 10%, 15% and 20% loading.

The FT-IR spectra shown in figure 5 confirmed the presence of styrene, n-octadecane and PVA in PVA nanofibres loaded with

PS/n-octadecane NCs. The peaks for aliphatic C-H stretching related to OD appeared at 2920 and 2852 cm^{-1} while aromatic C-H stretching of styrene was observed at 3000-3100 cm^{-1} . The peaks at 1460, 1375 cm^{-1} were associated with C-H bending vibrations of methylene bridge of n-octadecane and the peak at 720 cm^{-1} was associated with in-plane rocking vibration of CH_2 group of n-octadecane. The vibrations of aromatic C-H stretch were absent in n-octadecane and PVA nanofibres.

The SEM micrographs of control PVA (without NCs) and loaded PVA nanowebs are shown in figure 6. The average diameter of control PVA nanofibres obtained from 14 wt% solution was 403 ± 40 nm. It was observed that loaded PVA nanofibres had larger diameter. The diameter was found to vary considerably along the length because of the presence of NCs inside them. However, the diameters were still within the submicron range.

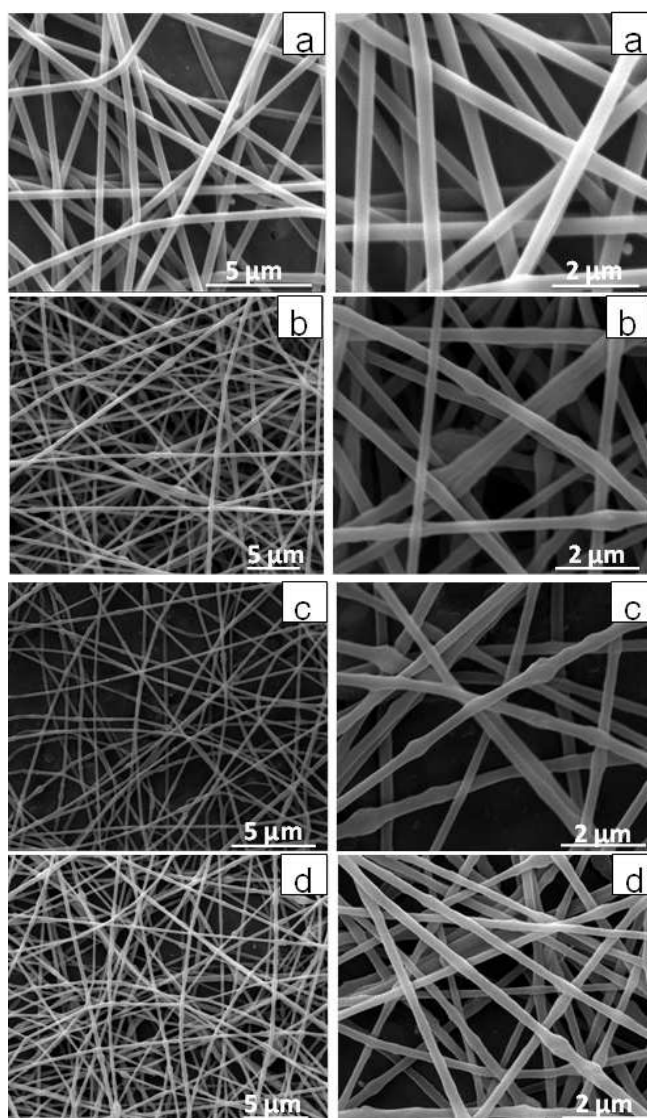


Figure 6. Surface morphology of electrospun PVA nanofibres at (a) 0%, (b) 10%, (c) 15% and (d) 20% OD loading on weight of PVA.

Table 2. Properties of PS/OD nanocapsule-loaded PVA nanofibres.

OD wt % (on the weight of PVA)	Avg. dia. of composite nanofibres (nm)		PVA conc. (w/w%)	Avg. dia. of PVA control (nm)	OD T _m (°C)	Latent heat of melting of composite fibres (J/g)	Latent heat of freezing of composite fibres (J/g)
	Bulged portion	Smooth portion					
-	-	-	14.0	403 ± 40	-	-	-
10	515 ± 94	323 ± 55	10.4	361 ± 84	25.0	2.2	-2.7
15	438 ± 100	292 ± 49	9.2	230 ± 22	25.3	4.3	-4.8
20	425 ± 93	264 ± 35	8.3	204 ± 34	24.8	3.3	-4.0

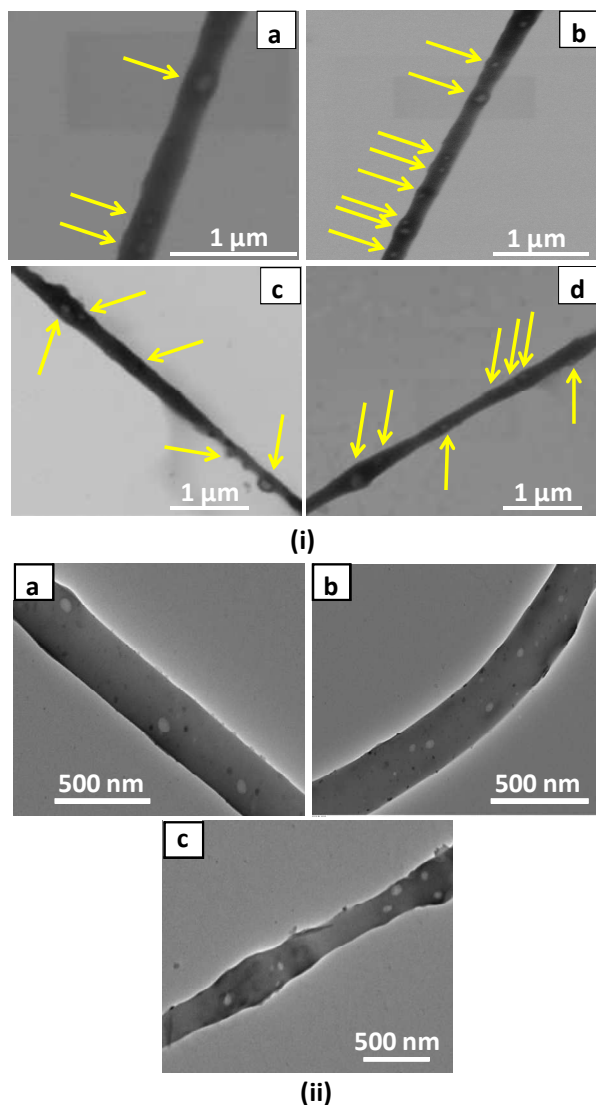


Figure 7. (i) STEM (ii) HRTEM micrographs of PCM loaded PVA nanofibres (a) 10%, (b) 15%, (c & d) 20% OD loading on the weight of PVA. Arrows show the presence of NCs.

The average diameter of nanofibres in loaded region was 515 ± 94 nm for 10 wt% OD loading. This decreased to 425 ± 93 nm as the OD loading was increased from 10 to 20 wt% (Table 2). The presence of NCs and their association with PVA polymeric chains is likely to increase the elasticity of the composite

solutions, and is thus, primarily responsible for the increase in diameter of nanofibres even at lower concentration of PVA in comparison to the control PVA.

The diameter of the smooth portions was found to be a little lower for nanofibres with 10 wt% loading compared to that of control PVA. This may be attributed to the fact that the smooth portions of these fibres have none or fewer small sized NCs, compared to the bulged portions, which tend to incorporate more polymer in the bulged region. However, on increasing the loading to 15 and 20 wt%, several NCs and unfilled PS nanoparticles were also found to be present in the smooth portions, resulting in higher elasticity of the polymer solution, and hence, the higher diameter compared to the control PVA nanofibres.

Further, it was observed that as the loading was increased from 10 to 15 wt%, the frequency of occurrence of bulged portions also increased, which indicated increased concentration of NCs inside the nanofibres. On increasing the loading of OD to 20 wt%, the number of bulged portions further increased. However, the distribution of the portions was not even, which indicated that NCs could not be incorporated properly possibly because of the very low concentration of PVA at such high loading of OD.

The distribution of NCs inside the nanofibres was analysed using STEM and HRTEM imaging. The micrographs (shown in figure 7) of PCM loaded nanofibres revealed that NCs are present in both smooth and bulged portions. Smooth portions have fewer and smaller sized NCs, whereas the bulged portions have either bigger sized or larger number of NCs. At 10% loading, the nanofibres had good dispersion of NCs, though only a few, in the smooth portions. On increasing the loading of OD from 10 wt% to 15 wt%, the concentration of NCs in the nanofibres increased resulting in an increase of the number of bulged regions. The dispersion of NCs was still uniform in the smooth portions and the average distance among NCs had decreased. A small number of polystyrene particles were also observed inside nanofibres.

However, on further increasing the loading to 20 wt%, some of the NCs seemed to have moved towards the periphery of the nanofibres compared to that with 15 wt% OD. Moreover, a few NCs were also present on the surface and the dispersion was poorer with aggregated NCs resulting in nanofibres with distorted shapes. At 10% OD loading, $\sim 1.5 \pm 0.5$ NCs were incorporated per unit length (i.e. 1 μm) of nanofibre, while for 15% OD loading, the NCs increased substantially to $\sim 2.9 \pm 0.4$ NC/ μm . Further, on 20% loading, the occurrence of NCs inside the fibre could increase only marginally to $\sim 3.1 \pm 0.2$ NCs per μm , while a

large number of NCs, $\sim 1.5 \pm 0.5$ NC/ μm , were found adhering on the surface of nanofibres. In these fibres, the incorporated NCs were present in aggregated form. Therefore, 15 wt% was found to be the optimum loading concentration of OD in the PVA nanofibres.

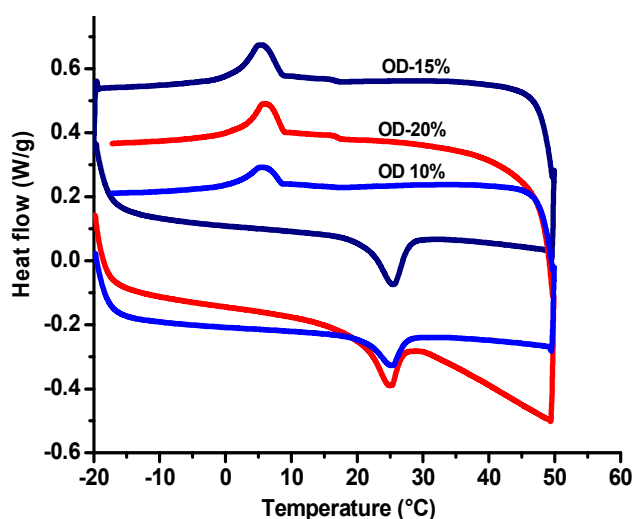


Figure 8. DSC thermographs of PVA nanofibres at 10, 15 and 20% OD loading.

DSC thermographs of n-hexane washed NCs loaded PVA nanofibres are shown in figure 8. In all the three cases, the phase change transition occurred at 25 ± 0.5 °C. The latent heat of fusion was maximum at 4.3 J/g for fibres with 15 wt% OD loading indicating that about 65% of the added NCs could be incorporated in the nanofibres. The results further confirmed that NCs could be incorporated inside the nanofibres and are well distributed. The latent of fusion was found to be decreased for 20 wt% loading, which further indicated that such a high concentration of NCs could not be properly incorporated in the nanofibres.

4. Conclusions

Uniform sized PS/OD NCs were synthesized using SM-RAFT miniemulsion polymerization technique. These PS/OD NCs could be successfully incorporated inside PVA nanofibres using electrospinning technique to form composite nanofibres. The presence of NCs inside nanofibres was confirmed by FT-IR analysis. Morphological studies on FE-SEM and STEM/HRTEM showed that the NCs were dispersed within nanofibres. The dispersion and distribution of NCs was better at 15% OD loading and the average diameter of loaded and unloaded regions was in submicron range at 438 nm and 292 nm, respectively. The PS/OD loaded PVA nanofibres absorbed 4.3 J/g heat at 25.3 °C and released 4.8 J/g at 9.2 °C, indicating that about 65% of the added NCs were incorporated. The technique offers a method of making composite nanofibres loaded with encapsulated materials suitable for various applications.

Acknowledgements

The authors acknowledge partial financial support provided by Department of Science and Technology, Govt. of India under various research grants. One of the authors (S.Sirohi) would like to thank Bhaskaracharya College of Sciences (University of Delhi) for providing opportunity to pursue Ph.D. under which this work was carried out.

Notes and references

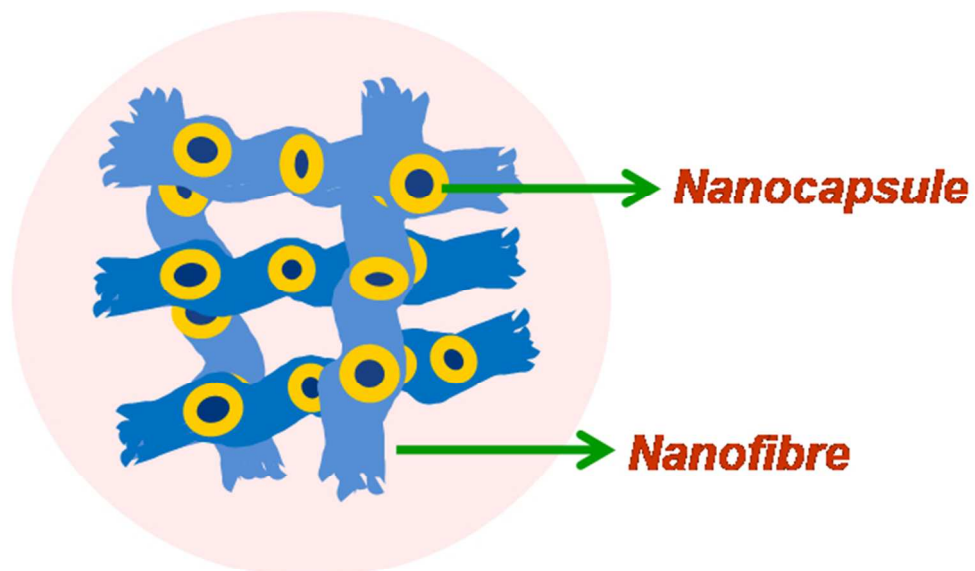
⁵⁰ ^a Address: SMITA Research Lab, Department of Textile Technology, Indian Institute of Technology, Hauz Khas, New Delhi 110016, India, Tel: +91-11-26591426, 26591415; E-mail: manjeet.jassal@smita-iitd.com; ashwini@smita-iitd.com

⁵⁵ [†] Electronic Supplementary Information (ESI) available: [recipe of PS/OD NCs, latex photograph, FE-SEM micrographs of composite PVA nanofibres at 20% OD loading, control PVA nanofibres and details of calculations]. See DOI: 10.1039/b000000x/

⁶⁰

1. D. Li and Y. Xia, *Advanced materials*, 2004, **16**, 1151-1170.
2. G. C. Rutledge, *Journal of Physics: Conference Series*, 2008.
3. S. Basu, A. K. Agrawal and M. Jassal, *Journal of Applied Polymer Science*, 2011, **122**, 856-866.
- ⁶⁵ 4. D. Gupta, M. Jassal and A. K. Agrawal, *Industrial & Engineering Chemistry Research*, 2015, **54**, 1547-1554.
5. S. Basu, M. Jassal and A. K. Agrawal, *Journal of The Textile Institute*, 2013, **104**, 158-163.
6. J. Bai, Y. Li, S. Yang, J. Du, S. Wang, J. Zheng, Y. Wang, Q. Yang, X. Chen and X. Jing, *Solid State Communications*, 2007, **141**, 292-295.
7. A. Greiner and J. H. Wendorff, *Angewandte Chemie International Edition*, 2007, **46**, 5670-5703.
8. S. Tan, X. Huang and B. Wu, *Polymer International*, 2007, **56**, 1330-1339.
- ⁷⁵ 9. Y.-H. Yu, C.-C. Chan, Y.-C. Lai, Y.-Y. Lin, Y.-C. Huang, W.-F. Chi, C.-W. Kuo, H.-M. Lin and P.-C. Chen, *RSC Advances*, 2014, **4**, 56373-56384.
10. A. Daneleviciute-Vaisniene, J. Katunskis and G. Buika, G. Buika, *Fibres & Textiles in Eastern Europe*, 2009, **17**, 40-43.
- ⁸⁰ 11. C. A. Bessel, K. Laubernds, N. M. Rodriguez and R. T. K. Baker, *The Journal of Physical Chemistry B*, 2001, **105**, 1115-1118.
12. H. Ye, N. Titchenal, Y. Gogotsi and F. Ko, *Advanced materials*, 2005, **17**, 1531-1535.
- ⁸⁵ 13. G. L. Bezemer, J. H. Bitter, H. P. C. E. Kuipers, H. Oosterbeek, J. E. Holeyijn, X. Xu, F. Kapteijn, A. J. van Dillen and K. P. de Jong, *Journal of the American Chemical Society*, 2006, **128**, 3956-3964.
- ⁹⁰ 14. N. M. Rodriguez, M.-S. Kim and R. T. K. Baker, *The Journal of Physical Chemistry*, 1994, **98**, 13108-13111.
15. S. Agarwal, J. H. Wendorff and A. Greiner, *Polymer*, 2008, **49**, 5603-5621.
16. D.-G. Yu, L.-M. Zhu, K. White and C. Branford-White, *Health*, 2009, **1**, 67-75.
- ⁹⁵ 17. X. Xing, Y. Wang and B. Li, *Opt. Express*, 2008, **16**, 10815-10822.
18. R. Nain, M. Jassal and A. K. Agrawal, *Composites Science and Technology*, 2013, **86**, 9-17.
- ¹⁰⁰ 19. H. Yoshimoto, Y. M. Shin, H. Terai and J. P. Vacanti, *Biomaterials*, 2003, **24**, 2077-2082.
20. I. Uslu, T. Tunc, M. Öztürk and A. Aytimur, *Polymer-Plastics Technology and Engineering*, 2012, **51**, 257-262.

-
21. A. L. Yarin, E. Zussman, J. Wendorff and A. Greiner, *Journal of Materials Chemistry*, 2007, **17**, 2585-2599.
22. W. Salalha, Y. Dror, R. L. Khalfin, Y. Cohen, A. L. Yarin and E. Zussman, *Langmuir*, 2004, **20**, 9852-9855.
- 5 23. S. Alay, F. Göde and C. Alkan, *Fibers Polym*, 2010, **11**, 1089-1093.
24. R. Faridi-Majidi, M. Madani, N. Sharifi-Sanjani, S. Khoei and A. Fotouhi, *Polymer-Plastics Technology and Engineering*, 2012, **51**, 364-368.
- 10 25. M. Barari, R. Faridi-Majidi, M. Madani, N. Sharifi Sanjan and M. A. Oghabian, *Journal of Nanoscience and Nanotechnology*, 2009, **9**, 4348-4352.
26. S. Basu, N. Gogoi, S. Sharma, M. Jassal and A. K. Agrawal, *Fibers Polym*, 2013, **14**, 950-956.
- 15 27. S. Basu, M. Jassal and A. K. Agrawal, *Journal of The Textile Institute*, 2013, **104**, 1071-1079.



Composite nanofibre

115x75mm (150 x 150 DPI)